Reply to Referee #1

We would like to thank the referee for his/her valuable and detailed comments. Our answers to the comments are given below in blue letters, while the referee comments are given in black italics. Additionally we added the changes we would like to make in the revised manuscript in blue bold letters.

1) *Regarding the retrieval of the RI; The retrieval of the RI in the laboratory is done by size selecting several diameters, an RI is retrieved for every size, and then the average RI of all the sizes is taken as the final retrieved RI and compared to literature data. For PSL, four different sets of measurements were done with a mean RI = 1.60 (±0.04), but if you look specifically at the RIs from a single diameter, for example 500nm, the RI varies from 1.55 to 1.6 for the two data points shown. For a 300nm diameter the RI varies from 1.53 to ~1.625. These variations are larger than the stated error.*

   Indeed, the single data point error is larger than the stated ±0.04. The uncertainty that we give is ±σ (± one standard deviation) while single data points may still fall outside of this range.

   Revised text: Page: 7341; line: 19-21:
   The retrieved index of refraction for PSLs was found to be m=1.60±0.04 (mean ± 1 SD) which agrees well with the literature value of m≈1.59 (see Sect. 2.2.1).

2) *This RI is then taken as an input variable to obtain the GF. The authors do not show how these variations for retrievals done with a single diameter are reflected in the GF calculations, specifically of the error.*

   This is true; the sizing uncertainties shown in Fig. 8 of the ACPD version of our manuscript are not applicable for the optical sizing of growing solution droplets, as it is derived from Mie curves for a size-independent index of refraction. Therefore, we want to add an additional figure with an associated discussion which quantifies the sizing uncertainty for growing solution droplets (Sect. 3.1.2). Additionally, we have improved the previous Fig. 8 (see Fig. AR1 below) and added a new figure (see Fig. AR2 below) to better distinguish between absolute measurement uncertainty and repeatability, as well as an improved discussion of uncertainties associated with ambiguities in the Mie curves.

Revised text: Page: 7340; line: 20- end of section 3.1.2:
To retrieve the uncertainty in the optical diameter measurement, the 15% uncertainty (1 SD) of the scattering cross section measurement is used as input for error propagation calculations. This uncertainty is present despite the calibration with Caldust and is referred to as "calibration uncertainty" from now on. On the other hand recurrent measurements of monodisperse ammonium sulfate particles revealed that the random uncertainty describing the repeatability of the measurements amounts to less than 2% (1 SD; referred to as "repeatability uncertainty" from now on). Figure 8 depicts the absolute values of the resulting estimated relative uncertainty of the optical diameters for four different indices of refraction: 1.59, 1.50, 1.40 and 1.33, representing PSL, the range often found for atmospheric aerosol and pure water, respectively. The uncertainty for optical diameters, resulting from a fixed uncertainty in the scattering cross section, depends on the local gradient of the Mie curve and thus on the particle size and index of refraction. This explains why the relative sizing uncertainty shown in Fig. 8 strongly depends on diameter and index of refraction. It is clearly visible that the influence of the calibration uncertainty dominates, resulting

in an average relative sizing uncertainty of 9% for these indices of refraction in the range between 300 nm and 1 µm, with minimal and maximal values of 4% and 22%, respectively, for m = 1.50 at 0.469 µm and m = 1.33 at 0.300 µm. The repeatability uncertainty amounts on average to 1.6% (dashed lines in Fig. 8) and therefore plays a minor role (for measurements with sufficient counting statistics). The error analysis presented in Fig. 8 is only valid if particles have a constant index of refraction, e.g. for the optical sizing of a dry aerosol sample.

The Mie curves (green lines in Fig. 4) for solution droplets that grow by absorption of water are less steep than those for a constant index of refraction (red and blue curves in Fig. 4). Hence, for particles growing by water uptake the sizing uncertainty has to be calculated with respect to these curves. The solid lines in Fig. 9a-b are equivalent to those in Fig. 4 but for using a dry index of refraction of 1.50. The Mie curves for solution droplets with a dry size of 300 nm, solid green lines in Fig. 9a, have a local maximum at GF = 1 and a local minimum at GF = 1.2. This results in sizing ambiguities for solution droplets with a scattering cross section value in between those of the local extremes, i.e. for the growth factor range GF < 1.4. This "ambiguity uncertainty" is shown as red shading in Fig. 9c. For particles with a true GF of 1.0 < GF < 1.2 (range between the positions of the local extremes), the ambiguity can potentially result in an over- or under sizing, while for particles with GF between 1.22 and 1.4 the ambiguity results in potential under sizing. The associated relative uncertainty is larger than ±20%. Therefore we only report data for GF>1.4 in the case of 300 nm particles. A small ambiguity uncertainty also occurs for GF>4.8, which is only relevant for very hygroscopic particles at very high relative humidity. For the 500 nm particles an ambiguity uncertainty of mostly <~6% occurs in the range GF ≤ 2.8 for particles with m_{dry}=1.50 (Fig. 9d). In case of higher m_{dry}, ambiguity also becomes an issue in the range GF <~1.15 (see dashed green line in Fig. 4a).

The repeatability of the calibrated scattering cross section measurements with the WELAS is ~±2% (1 SD; see Sect. 3.1.2). The associated sizing uncertainty (violet curves in Fig. 9c-d) is obtained by changing the scattering cross section σ_s by ±2% (in order to separate the uncertainties due to different causes, the Mie curves were smoothed in the upper GF range before inferring the "repeatability uncertainty" and the "calibration uncertainty"). The repeatability typically causes less than 3% sizing uncertainty, except for D_{dry}=500 nm and GF<1.4, where this uncertainty increases by up to 6% due to the lower gradient of the Mie curve. More relevant than the repeatability uncertainty is the absolute calibration uncertainty of the scattering cross section measurement by the WELAS (1 SD = ±15%; see Fig. 7 and discussion above). An absolute calibration bias is partially accounted for by adjusting the index of refraction of the dry particles according to the dry mode WHOPS measurement. This ensures that no sizing bias occurs at GF=1 (cf. blue curve in Fig. 9d). However, the Mie curves for the adjusted index of refraction (dashed and dashed dotted green lines in Fig. 9a-b for m_{dry} = 1.53 and 1.47 and m_{dry} =1.53 and 1.46, respectively), have a slightly different slope than the "true" Mie curve for m_{dry} = 1.50, such that a calibration bias still causes a sizing uncertainty for GF>1. Comparing all uncertainties reveals that the calibration uncertainty, which causes a sizing uncertainty of up to ±10% for GF<3.3, is the dominant source of uncertainty, except for GF<~1.4, where the ambiguity uncertainty dominates for D_{dry}=300 nm (any m_{dry}).

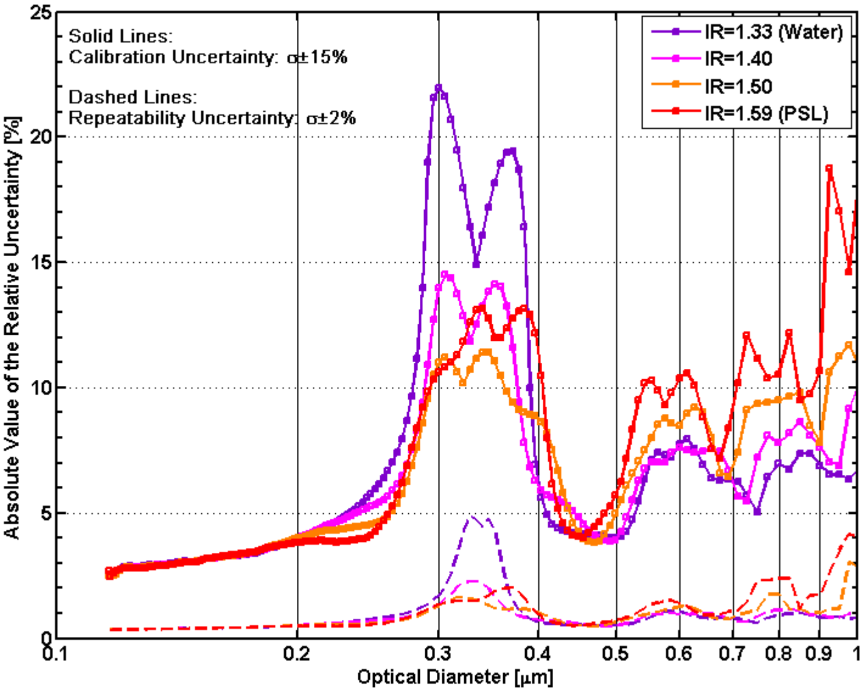

Figure AR1: New version of Fig. 8;

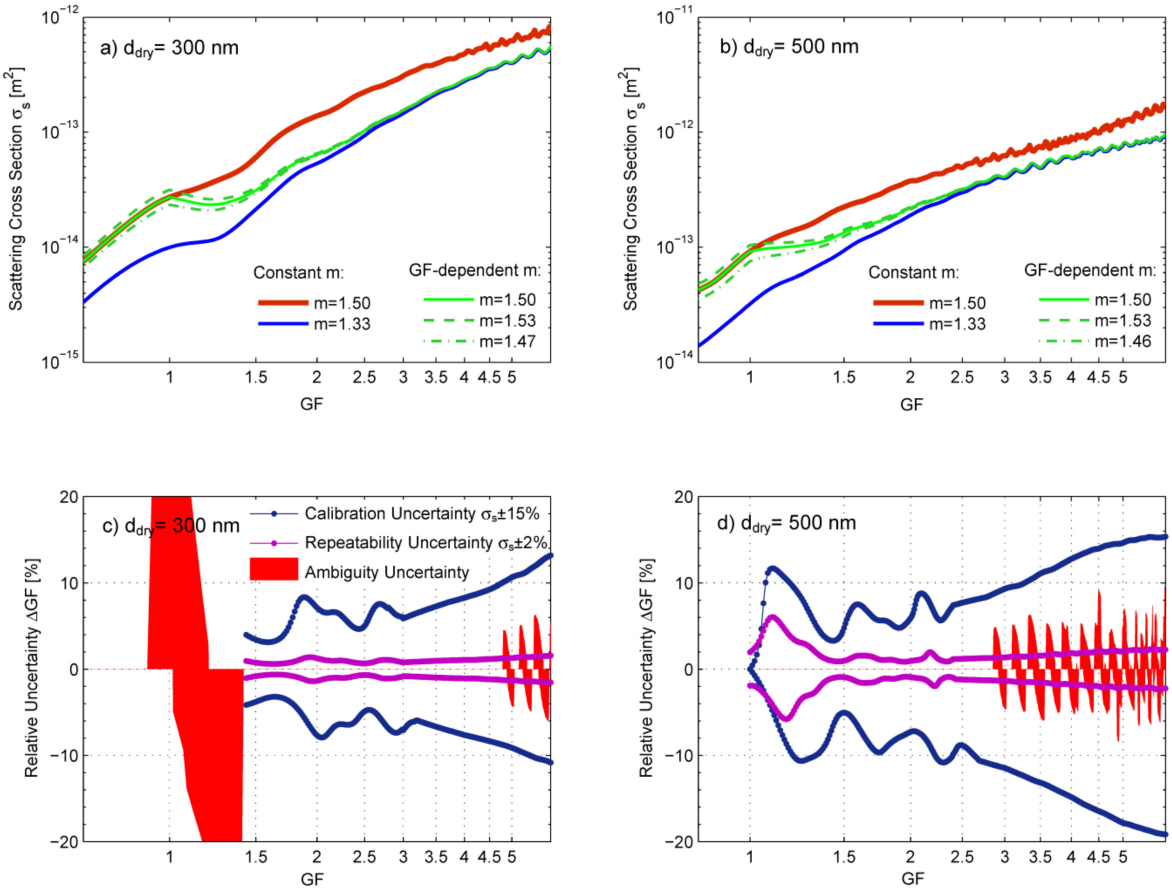

Figure AR2: Additional Fig. (new Fig. 9) to describe the relative uncertainty with regard to the GF measurements

.

Caption for new Fig. 9 (added to the revised manuscript):

Optical sizing of solution droplets. Panels a and b show theoretically calculated scattering cross section versus growth factor (solid green lines) for the example of particles with a dry index of refraction of 1.50 and dry diameters of 300 and 500 nm, respectively. The solid red and blue lines are theoretical curves for particles with a constant index of refraction, and the green lines indicate the effect of a calibration bias (see text for details). Panels c and d display the sizing uncertainties due to different causes for the example particles from panels a and b, respectively.

Revised text: Page: 7348; line: 22:

For a constant index of refraction the uncertainty in the optical sizing was found to be ±9% while the uncertainty in the GF amounts to approximately ±10%.

3) *The authors even mention in page 7335 line 10-11: "Figure 4 demonstrates the crucial importance of using the appropriate index of refraction for the optical sizing of grown particles…"*

We were referring to the importance of accounting for the water absorption for the corresponding refractive index. The full sentence on p. 7335, line 10-11 reads: "Figure 4 also demonstrates the crucial importance of using an appropriate index of refraction for the optical sizing of grown particles, in particular the need to account for the effect of absorbed water". The sensitivity to the index of refraction of the dry particles is now addressed with the new Fig. 9 added in response to the previous comment.

4) *Also, what is the convergence criterion for the RI retrieval using a single diameter? In their look up table(s) they look for a dry RI corresponding to a dry cross section and a GF=1, what is the interval between the 'steps' of the RI? In other words, do they vary the RI by 0.01 or 0.001? Also, can the authors state what wavelength range is the RI retrieval valid for?*

This is now clarified in the revised text: Page: 7333; line: 11-14
The data analysis step presented in box 2 of Fig. 3 provides the effective index of refraction ($m_{\mathrm{dry,meas}}$) of these dry particles, simply by searching the look-up table (which has a resolution of Δm=0.005 in the index of refraction) for the m_{dry} corresponding to $\sigma_{\mathrm{dry,meas}}$ for $D_{\mathrm{dry,mob}}$ and GF=1 (no hygroscopic growth in the dry mode).

5) *I also think the field measurement analysis of the Zeppelin campaign is missing important data to help the authors validate their proposed airborne system. The authors mentioned they had an Aerosol mass spectrometer (AMS), a Scanning mobility particle sizer (SMPS), an aethalometer, meteorological data from the zeppelin, and another WELAS to help validate their new system, but the data of these instruments was not used at all. The authors should incorporate the data from the additional instrumentation.*

The main topic of this paper is the technical description of the WHOPS instrument including technical design, data analysis procedures, uncertainty analysis and validation of accurate measurements – this was the very reason to choose AMT as a target journal for this manuscript as opposed to choosing a journal with a stronger focus on results and interpretation of atmospheric measurements such as e.g. ACP. Validation of new instruments is commonly done by the measurement of samples with known properties and behavior. In this case, PSL spheres and pure ammonium sulfate particles were used to validate the accuracy of optical sizing and hygroscopic growth factor measurements. Closure experiments, where the instrument response to a sample with a priori unknown behavior is compared against predicted behavior which is inferred from independent measurements of e.g. sample composition and by using a theoretical model, can only be used for instrument validation under certain conditions. The closure calculations proposed by the referee do not allow drawing any firm conclusions about the instrument performance; simply because the chemical characterization by the AMS is insufficient concerning a complete speciation (e.g. sea salt and dust components are not quantified). Therefore, we did not include such closure calculations. Nevertheless, the ambient measurements performed by the WHOPS were put in the manuscript to give an example about the kind of data that can be gathered during airborne measurements with the WHOPS. Comprehensive analyses of the aerosol and gas phase properties observed during PEGASOS flights in the context of air mass properties, vertical layering etc. are the subject of papers that are currently in preparation.

6) *The authors mentioned that a change in wind direction “obviously” demonstrates a change in air mass. I think the authors should show a full meteorological analysis to support this claim. They can show wind speed, temperature, RH, particle concentration, and size distributions from the SMPS. If wind direction alone can indicate a change in air mass then the changes seen at the beginning of the campaign, between 14:55 and 15:30, will also have to be changes of air mass. Fig.11c should have wind speed in the left y-axis and the wind direction can be depicted with arrows, with a separate arrow showing what direction signifies north.*

Figure 12 (= Fig. AR3 here = Fig. 11 in AMTD manuscript) has been adapted (e.g. wind speed and wind direction with arrows and particle number concentration) to support the statement for a change in air mass. Since the time series of the temperature and RH did not show any main variations, except for the one when the flight altitude is increased which is also visible in the particle number concentration, we chose not to add them.

Revised text: Page: 7345; line: 5-20

The time series of the measured mean GFs and κ-values for 500 nm particles are shown in Fig. 12e (black curve). The error bars indicate the measurement uncertainty of ±10% (1 SD; see Sect. 3.1.2). Higher κ-values (median=0.55) were found during the first part of the flight, when the Zeppelin headed inland towards Cabauw and back to Rotterdam (from now on referred to as “Part 1”), while lower κ-values (median=0.31) were found during the second part of the flight which was directed towards the sea and back to Rotterdam (from now on referred to as “Part 2”). The prevailing local wind direction (arrows in Fig. 12c), measured on board the Zeppelin NT, differed clearly between these two regions (the change in local wind direction is marked by the dashed, grey line): during “Part 1”, north-westerly winds were dominant, while during “Part 2” north-easterly winds prevailed. Besides, the wind speed is illustrated in Fig. 12c, showing generally low

values (2-4 ms^{-1}). The number concentration of particles with D>300 nm obtained from the polydisperse WELAS measurement (turquoise line in Fig. 12d) increases sharply just after the local wind direction changes. This gives clear evidence that the Zeppelin NT entered a different air mass during the second part of the flight.

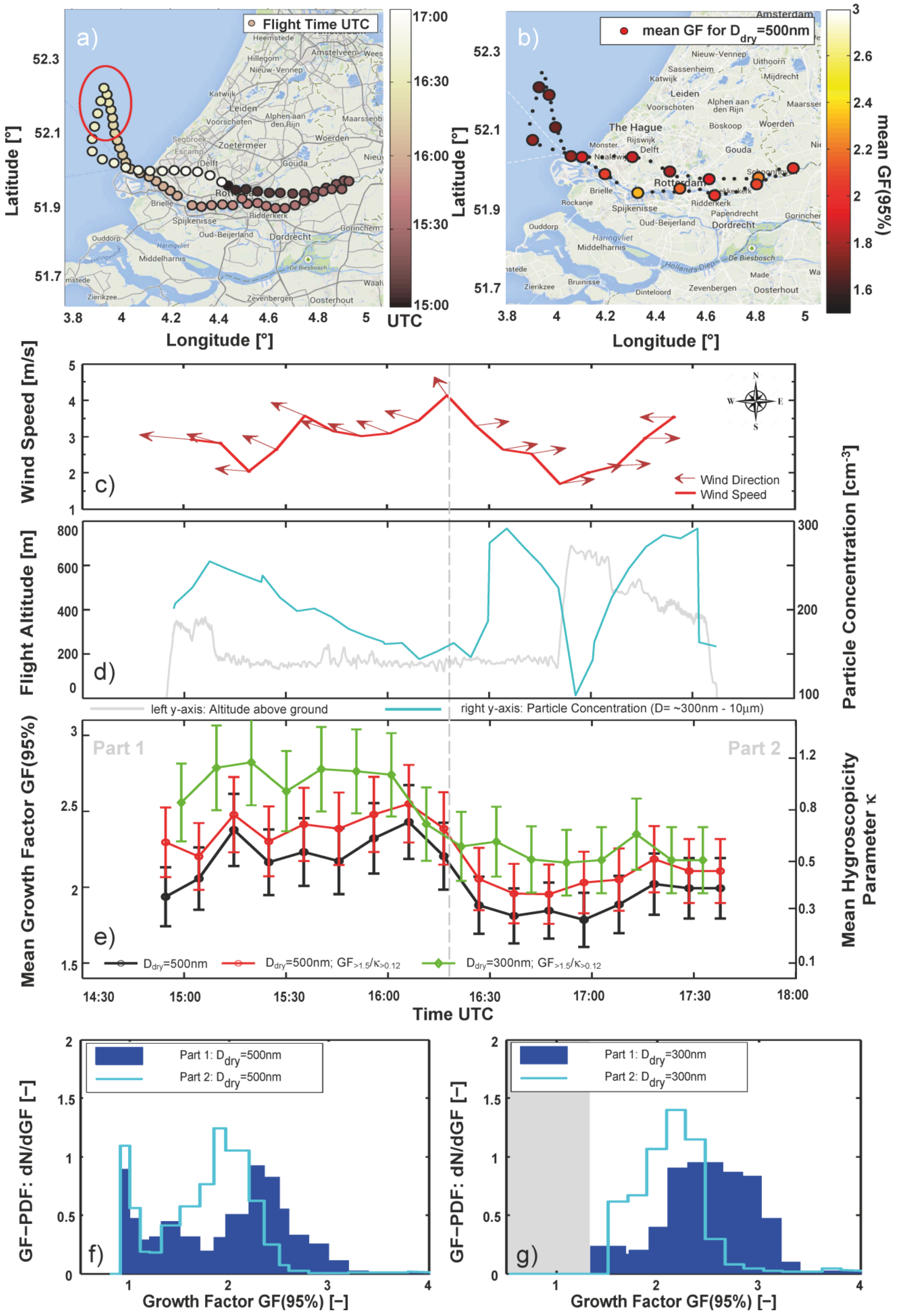

Figure AR3 = new Fig. 12 (replacing previous Fig. 11): new version of Fig. 11 (now Fig. 12)

Adapted figure caption:

Example of an airborne WHOPS measurements onboard the Zeppelin NT from 22 May 2012 in the Netherlands; (a) flight track color coded by UTC time; (b) mean GFs (color-coded) at RH=95% for D_{dry}=500 nm particles; (c) time series of the local wind speed (red curve) and wind direction (red arrows) measured on board of the Zeppelin NT; (d) time series of the flight altitude (gray line) and number concentration of particles with D>300 nm measured by the polydisperse WELAS1 (turquoise line); (e) time series of the measured mean GF (left axis) and corresponding κ-values (right axis) for the selected particle size of 500 nm; additionally the mean GF of all particles with $GF_{>1.5}$ ($\kappa_{>0.12}$; lower detection limit when selecting 300 nm particles) is shown for the 300 nm and 500 nm particles; the gray dashed line across panels (c) , (d) and (e) marks the point in time when the local wind direction changed between the first and second part of the flight; (f) GF-PDF for humidified 500 nm particles separately averaged over "Part 1" and "Part 2"; (g) equivalent to (f) but showing results for 300 nm particles; the gray area covers the GF range that cannot be reliably detected for this particle size.

7) *The authors mentioned that Fig. 11d shows the measured mean GF and kappa values (black line) for 500nm particles. The authors need to show the error bars. If what the authors define as Part 1 is the same are mass, how do they explain the large variations from a mean GF ~ 1.7 to a mean GF ~2.6? How can a variation from a GF~2.3 to a GF~3 occur in what looks as two consecutive measurements (See Fig. 11b at 51.9N – 4.6E)? I think the SMPS and AMS data can help resolve this issue, by providing the concentration and chemical composition of the particles (and specifically the concentration of the 500nm particle), respectively.*

Error bars have been added to the revised Figure. Unfortunately, there was also a small error in the analysis procedure for the raw data for those sizes and GFs where ambiguities between scattering cross section and particle diameter occur. We have corrected all data presented in this paper for this error. This had very little effect in most cases, while a few data points changed by up to 10 %. After this correction, the difference in the hygroscopic properties of the particles between the two air mass types becomes much more consistent (see new Fig. 12e = Fig. 3 in this author reply). Furthermore, we adapted Fig. 12b now showing 300s averages instead of 50s averages in order to avoid artificial variability due to limited counting statistics. The addition of further data to Fig. 12 to support the air mass change has already been addressed with the reply to the previous comment.

8) *Also, the authors should better explain the purpose of adding mean growth factor of particles larger than 1.5 in Fig. 11d (red and green lines).*

Ideally, a comparison between particles with 300 and 500 nm dry diameter would be done for the complete hygroscopicity distribution. However, only the hygroscopic particles with GF>1.5 can be measured with the WHOPS for particles with a dry diameter of 300 nm. Therefore, only the properties of the hygroscopic particle fraction could be compared between the particles with dry diameters of 300 and 500 nm. Besides, the comparison of the overall mean GF with the mean GF of the hygroscopic particles at a dry diameter of 500 nm provides information on the spatial distribution of the fraction of non- and weakly-hygroscopic particles.

Revised text: Page: 7347; line: 2-5:

For a spatially resolved comparison of the size dependence of particle hygroscopicity, Fig. 12e additionally contains the mean GF of those particles with GF>1.5 for the dry diameters 300 nm (green symbols) and 500 nm (red symbols). This comparison reveals a similar spatial pattern with two distinct air mass types for both sizes. The mean GF values of the more hygroscopic particle fraction are just slightly larger at 300 nm dry diameter compared to 500 nm, as already seen from the GF-PDFs shown in Fig. 12f&g. However, this subtle difference is within the experimental uncertainty of the WHOPS (see error bars in Fig. 12e). The almost constant difference between the black and red lines in Fig. 12e further confirms that the change in the mean GF of the 500 nm particles between the two parts of the flight can mostly be attributed to a shift of the more hygroscopic mode with GF>1.5, while the number fraction and GF of the particles in the range GF<1.5 stayed quite constant over the whole flight, in agreement with Figs. 12f&g.

9) *The authors mention in page 7345 line 15-18 that they did back trajectory analysis, but that it is not possible to assign air mass types to the two parts they define. But the authors could define air mass type for certain measurements. For example, for the measurements taken at around latitude 52.5N – 3.9E, a back trajectory analysis can be done; see Fig. 1 below. Fig. 1Review shows that at both levels, 200m and 600m, the air mass arriving at the measurement point had been at least 12h above the sea. Hence, sea spray aerosol was most likely measured. The same can be done for the aerosols that were measured at the beginning of the campaign. From Fig.2Review, the aerosols that were measured at 15:00 (the beginning of the campaign) had more continental influence than the ones measured at 17:00. From Fig. 11b in the paper, the GFs measured at the two points shown in Fig1Review and Fig.2Review have approximately the same value GF~1.8, can the authors explain this? This quick analysis can of course be greatly improved (e.g., using the AMS, SMPS, wind speed and direction, etc.), but I think the authors need to show that the results given by the WHOPS are consistent.*

Based on the back trajectory analysis that we had done, we came up with the same conclusion as the referee, concerning potential influence from sea salt or continental aerosol for the two parts of the flight. However, the GF results from the WHOPS show the opposite trend to what could be expected based on this back trajectory classification. Furthermore, the back trajectory simulations are inconsistent with the measurement of the local wind direction displayed in Fig. 12c, and regional aerosol sources can possibly also have had a substantial influence, due to fairly low wind speeds during the whole flight (2-4 m/s). Therefore, we conclude that the Hysplit model simulations, which may have missed regional flow patterns such as e.g. land-see breeze effects, cannot be used for a reliable air mass classification in our case.

Conclusive consistency checks of the WHOPS measurements against the chemical composition data are not possible as the AMS cannot quantify sea salt and dust components. Therefore, we chose to remain purely descriptive and to put our airborne results in the context of previous more comprehensive ground-based hygroscopicity measurements at the Cabauw site (see Table 1 and associated discussion).

Revised text of Page: 7345; line: 15-18:

Back trajectory analysis (not shown) was performed for different places and time periods and revealed that the probed air masses had maritime and/or continental influences. However, the whole flight was dominated by low wind speeds (2-4 ms^{-1}) and changes in the local wind direction were not captured by the Hysplit model such that the model output was not reliable.

10) *The authors mention that on average 15% of the particles had GF < 1.1, which could be explained with externally mixed dust, soot, or biological particles. Here, for example, they could use the aethalometer data to verify the influence or non-influence of soot.*

Unfortunately, the aethalometer neither provides size-resolved data nor mixing state information, which would be required to verify the potential (non-)influence of soot. We adapted the discussion as follows:

Revised text: Page: 7345; line: 26-29:
On average, about 15% of 500 nm dry particles had GF<1.1, which could be explained with externally mixed dust (e.g. Herich et al., 2009), fresh soot (e.g. Tritscher et al., 2011) or biological particles (e.g. Després et al., 2012). Mineral dust and possibly biological material are more likely, as the size distribution of such particles is known to extend down to the submicron size range (Després et al., 2012;Mahowald et al., 2014), while fresh soot particles typically show up at smaller sizes (~100 nm; Rose et al., 2006).

11) *What was the average number of particles measured to obtain the RI and GF for the two diameters used?*

Revised text: Page: 7336; line: 23:
The selected dry diameters were D_{dry} =300 and 500 nm. In order to get accurate, effective indices of refraction and mean growth factors, the mean values were calculated from 70 particles on average. According to the sensitivity analysis provided in Gysel et al. (2009),this is sufficient to avoid additional noise from limited counting statistics.

12) *Why do the authors use a log scale in the x-axis of Fig.11e and Fig.11f? Also, why is dN/dlogGF used? Are the widths of the GF bins different? What are the widths? If they are, this should be mentioned in the method section, and explain why there is a need for different widths in the GF measurements.*

The log scale was originally chosen to better display the values. However, we switched to a linear scale now, as the difference is actually small. Using regular or irregular bin widths is irrelevant, when choosing appropriate units for the y-axis (counts per bin would not be appropriate). More important, for easy interpretation of the graph, is to choose the units in such a manner that an equal area below the curve means an equal number fraction out of the whole sample, i.e. dN/dGF combined with a linear GF scaling (adapted Fig. 11; now Fig. 12) or dN/dlogGF combined with a logarithmic GF scaling (previous Fig. 11). The GF bins in our figures are irregular for several reasons: The WELAS returns the particle size distributions with regular size bins on a logarithmic scale. Recalculating the particle sizes to the correct index of refraction then results in irregular size bins. We further merged multiple size bins together in order to avoid an artificial fine structure in the size distributions that is simply an artefact resulting from sizing uncertainties rather than reflecting true aerosol properties.

13) *The authors mentioned that they found a rather constant RI for the whole campaign, with a value of 1.42 (±0.04). However, they found a great variability in the GF. The variability in the GFs would imply different type of particles; wouldn't the authors expect a different RI as well? It is strange to have such a big variability in GF but a constant RI, can the authors elaborate on why the RI remained constant?*

A difference in GF does not necessarily imply a difference in RI. For example looking at organic and inorganic substances: their hygroscopic properties are very different while they can have similar indices of refraction.

14) *Would high concentrations of NOx or O3 affect the measured diameter in the WELAS? Were high concentrations of NOx and/or O3 encountered during the campaign?*

The path length of the light through sample air is by far too short (a few cm) to cause any significant interference from light absorption by NO_x or O_3, which would weaken the light scattering signal.

15) *Was the counting efficiency experiment done with the 0.5lpm WELAS or the 5.0lpm WELAS? Would the nozzle that the company inserted make a difference?*

The counting efficiency experiment was done for the 0.5 lpm WELAS (WELAS2) which is part of the WHOPS, while the WELAS running on 5lpm was just an additional instrument on board of the Zeppelin. The nozzle was inserted to better guide the particles towards the measurement volume thereby increasing the detection probability.

Revised text: Page: 7336; line: 1:
The size-resolved counting efficiency (CE) of the WELAS2 (situated in the WHOPS) was tested...

16) *When deriving the RI from a single diameter, was Ddry,mob assumed to be one diameter, or was a narrow size distribution used? Is there a difference in the retrieved RI?*

We simply used the nominal dry diameter; however, we performed also sensitivity studies with a narrow size distribution (see Sect. 3.1.2, page 7339 line 28 and page 7340 lines 1-4).

Revised text: Page: 7330; line: 6:
A DMA-selected aerosol sample has a finite width rather than being perfectly monodisperse. Thus Eq. (6) should also be averaged over the size distribution of the quasi-monodisperse sample. However, we simply used the nominal dry diameter ($D_{dry,meas}$) for the Mie calculations. This does not introduce significant errors for polychromatic light, as averaging over wavelength or size has similar effects.

17) *I don't think the authors should use the qualifiers: "more hygroscopic", "non- or slightly hygroscopic", etc. It is ambiguous. They can just say 74% of the particles had GF > 1.5, for example.*

All these expressions were replaced by "…xx% of the dry 500 nm particles had GFxx…".

18) *Page 7325, line 20: Add the country to the WELAS description*

Revised text: Page: 7325; line: 19-20:
A WELAS 2300 sensor (white-light aerosol spectrometer; Palas GmbH, Karlsruhe, Germany)…

19) *Page 7327, line 16: Add company, city, model, country, etc. –*

Revised text: Page: 7327; line: 16:
We use HC-S probes (hygroclip – S; Rotronic AG, Bassersdorf, Switzerland)…

20) *Page 7328: What is PROMO?*

The Promo is the box containing the light source and photomultiplier connected to the WELAS sensor. This was introduced in page 7326, line 17. To avoid confusions it is called the same way in page 7328.

Revised text: Page: 7328; line: 25:
The pulse height recorded as a raw voltage (V_{raw}) by the PMT situated in the "PROMO 3000 box", which …

21) *Page 7332, lines 18-20: Hand and Kreidenweis (2002) should be added, they also have a similar approach*

Revised text: Page: 7332; line: 18-20:
A similar approach was described in previous articles like in Flores et al. (2009) for WELAS measurements or in Hand and Kreidenweis (2002).

22) *Page 7342, line 7: 'vales' should be 'values'*

This mistake will be corrected in the revised version.

23) *Page 7344, line 13: change 'nm' to 'm'*

This mistake will be corrected in the revised version.

24) *Page 7345, line 6: 'Fig. 11c' should be 'Fig. 11d'. Line 19: 'Fig. 11d' should be 'Fig. 11e'*

This mistake will be corrected in the revised version.

25) *Page7364, Fig.10a. The legend is wrong. 'ADDEM' is shown for the measured GF.*

This mistake will be corrected in the revised version.

26) *Page 7365-7366. Why does Fig. 11 have two captions? Maybe it will be better to put the 'second' Fig. 11 as Fig. 12?*

This is now a single figure (Fig. 12) with single caption after switching to AMT format.

References:

Després, V. R., Huffman, J. A., Burrows, S. M., Hoose, C., Safatov, A. S., Buryak, G., Fröhlich-Nowoisky, J., Elbert, W., Andreae, M. O., Pöschl, U., and Jaenicke, R.: Primary biological aerosol particles in the atmosphere: a review, Tellus B, 64, 2012.

Flores, J. M., Trainic, M., Borrmann, S., and Rudich, Y.: Effective broadband refractive index retrieval by a white light optical particle counter, Physical Chemistry Chemical Physics, 11, 7943-7950, 2009.

Gysel, M., McFiggans, G. B., and Coe, H.: Inversion of tandem differential mobility analyser (TDMA) measurements, Journal of Aerosol Science, 40, 134-151, http://dx.doi.org/10.1016/j.jaerosci.2008.07.013, 2009.

Hand, J. L., and Kreidenweis, S. M.: A new method for retrieving particle refractive index and effective density from aerosol size distribution data, Aerosol Science and Technology, 36, 1012-1026, 10.1080/02786820290092276, 2002.

Herich, H., Tritscher, T., Wiacek, A., Gysel, M., Weingartner, E., Lohmann, U., Baltensperger, U., and Cziczo, D. J.: Water uptake of clay and desert dust aerosol particles at sub- and supersaturated water vapor conditions, Physical Chemistry Chemical Physics, 11, 7804-7809, 10.1039/b901585j, 2009.

Mahowald, N., Albani, S., Kok, J. F., Engelstaeder, S., Scanza, R., Ward, D. S., and Flanner, M. G.: The size distribution of desert dust aerosols and its impact on the Earth system, Aeolian Research, 15, 53-71, http://dx.doi.org/10.1016/j.aeolia.2013.09.002, 2014.

Rose, D., Wehner, B., Ketzel, M., Engler, C., Voigtländer, J., Tuch, T., and Wiedensohler, A.: Atmospheric number size distributions of soot particles and estimation of emission factors, Atmos. Chem. Phys., 6, 1021-1031, 10.5194/acp-6-1021-2006, 2006.

Tritscher, T., Juranyi, Z., Martin, M., Chirico, R., Gysel, M., Heringa, M. F., DeCarlo, P. F., Sierau, B., Prevot, A. S. H., Weingartner, E., and Baltensperger, U.: Changes of hygroscopicity and morphology during ageing of diesel soot, Environmental Research Letters, 6, 10.1088/1748-9326/6/3/034026, 2011.